

# Exciton Dynamics on Rubrene (001) Crystal Surfaces with Microstructure Confinement

R. J. Stöhr,<sup>1</sup> G. J. Beirne,<sup>2</sup> P. Michler,<sup>2</sup> R. Scholz,<sup>3</sup> J. Wrachtrup,<sup>1</sup> and J. Pflaum<sup>1</sup>

<sup>1</sup>*3. Physikalisches Institut, Universität Stuttgart, 70550 Stuttgart, Germany*

<sup>2</sup>*Institut für Halbleiteroptik und Funktionelle Grenzflächen, Universität Stuttgart, 70550 Stuttgart, Germany*

<sup>3</sup>*Walter Schottky Institut, Technische Universität München, 85748 Garching, Germany*

(Dated: May 29, 2019)

The exciton dynamics on flat (001) rubrene crystal surfaces have been compared with those under confined pyramidal geometry by time-resolved photoluminescence with micrometer spatial resolution. The luminescence spectra can be interpreted in terms of generation of a free and a self-trapped exciton. Their ratio depends significantly on the structural size which we explain by the optical absorption profile of the pyramids in combination with the exciton diffusion constant. For the latter a lower limit of  $0.2 \text{ cm}^2/\text{s}$  at 4 K has been estimated. Temperature-dependent decay times reveal activation barriers between free and self-trapped exciton of 3 meV and 14 meV.

The optical properties of organic single crystals have been the subject of intense research for many decades. Their low symmetry and the correlation between their structural and optical properties result in complex phenomena such as Davydov-splitting, large hyperpolarizabilities and highly anisotropic optical parameters [1, 2, 3]. In contrast to their inorganic counterparts, the optical surface properties are not affected e.g. by dangling bonds. Furthermore, exciton binding energies of up to 1 eV favor the use of ordered molecular structures for opto-electronic applications at room temperature [4, 5]. However, fundamental aspects of the exciton formation, excitonic states and lifetimes are still not very well understood and are under discussion. The existence of a delocalized excitonic band versus the possible formation of a so-called "self-trapped" excitonic state, caused by the relaxation of the local molecular environment, highlights one of these key questions [6, 7]. In this context, the material dependent diffusion constants for the various excitonic species can only be estimated by laborious methods such as transient optical gratings on molecular crystals of high quality [8, 9].

In this Letter we describe a new approach to access the optical properties of ordered organic materials by analysing the exciton dynamics in self-organized pyramidal structures on the (001) rubrene crystal surface. Their regular arrangement and crystallinity prove to be beneficial for optical studies in contrast to approaches based on randomly oriented micro- and nanocrystals grown from precipitation [10]. The structural quality and the spatial extension enable the investigation of their optical characteristics in comparison with those of the planar (001) rubrene surface by photoluminescence with micrometer spatial resolution ( $\mu$ -PL). This information was complemented by data on the exciton formation and decay at various temperatures with picosecond resolution.

High quality rubrene crystals of orthorhombic symmetry were grown by sublimation under streaming  $\text{H}_2$  at a flow rate of 50 sccm. As rubrene is known to be highly suscep-

tible to photo-oxidation [11, 12] all samples were exposed to ambient conditions for times as short as possible. By Laue diffraction the crystal surface was estimated to be identical to the rubrene (001) plane. Optical microscopy yielded densities of  $5 \cdot 10^4 \text{ cm}^{-2}$  for the micron size self-organized pyramidal structures. Additional polarization studies corroborate that the microstructures are optically active and thereby indicate their crystallinity. Further structural analysis by AFM revealed a pyramidal baseline ratio of 2:1 in agreement with the ratio of the unit cell vectors of the (ab)-plane. The angles between the facets and the pyramidal base plane are about  $20^\circ$  along the [100] and  $16^\circ$  along the [010] direction. The resulting facets therefore roughly coincide with the low index planes of rubrene, such as, {103} and {013}. We will provide details of the underlying growth mechanisms leading to these structures in a forthcoming article.

For our  $\mu$ -PL experiments the rubrene crystals were mounted in a helium-flow cryostat that allows cooling to 4 K. The excitation wavelength of 380 nm was realized by using a frequency-doubled tunable Ti:Sapphire laser system providing 120 fs pulses at a repetition rate of 76 MHz. The laser emission could be focused by a long-working-distance 50x objective to a diameter of 1  $\mu\text{m}$ . Overall, lateral sample positioning within a resolution limit of 50 nm could be achieved. The optical and mechanical stability allowed for PL spectra to be measured even at different positions on an individual pyramid. The PL signal was spectrally resolved using a 0.75 m spectrometer. Time-integrated spectra were recorded with a liquid-nitrogen cooled CCD camera, while time-resolved experiments were performed by means of a fast avalanche photodiode with a time resolution of 40 ps.

The  $\mu$ -PL signals at 4 K recorded from several microstructures with different sizes are shown in Fig. 1 together with the luminescence signal emanating from the smooth rubrene surface (black curve). In total four peaks can be identified at 2.19 eV, 2.02 eV, 1.87 eV and 1.72 eV with their individual intensities varying as a function

of the respective pyramid size. Temperature variation from 4 K to 70 K exhibits a shift in the positions of the detected PL peaks by about 5 nm. In contrast, changing the applied laser power density from  $1 \mu\text{W}/\mu\text{m}^2$  to  $1000 \mu\text{W}/\mu\text{m}^2$  shows no such shift which leads us to the conclusion that local heating effects originating from the illumination can be neglected in further data analysis.

In the detected luminescence spectra an intensity en-

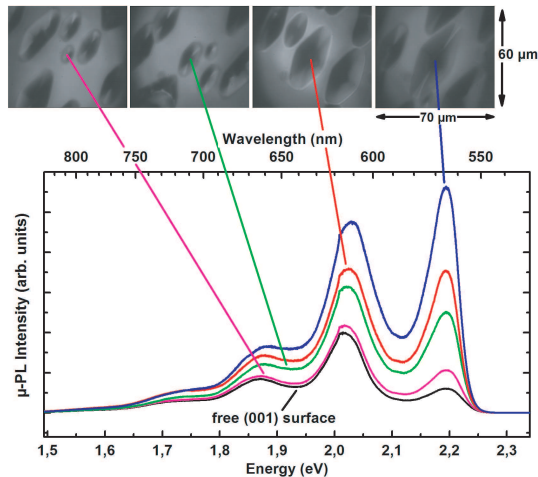


FIG. 1: PL signal recorded at 4 K from surface pyramids of various spatial extensions. The peaks can be attributed to a free exciton (2.19 eV) and a self-trapped exciton (2.02 eV) together with its vibronic replica (1.87 eV and 1.72 eV).

hancement is observed for all pyramidal structures with respect to the free rubrene surface. As a general tendency, the signals increase for larger structures. However, comparing the intensity evolution of the 2.19 eV peak with that of the three peaks at lower energies a different dependence on the pyramidal size can be assessed. This includes a pronounced shift in the relative intensity towards the PL at 2.19 eV for larger feature sizes as can be deduced from the blue and red curves of Fig. 1. To highlight this trend, we have estimated the ratio of the integrated intensities measured on the pyramids (ON) versus that on the flat rubrene crystal surface (OFF) for all peaks. In Fig. 2 the dependence of this quantity on the pyramid height is displayed for the four peaks. Evidently, the 2.19 eV band is enhanced by almost one order of magnitude with increasing structure size whereas the remaining three transitions appear to be only weakly affected by the geometrical dimensions. Furthermore, a critical structure size can be determined above which the integrated PL intensity is almost constant for all detected peaks. Before further analysis it is important to point out that we do not expect effects on the spectral signature from the oxidation products of rubrene, that emit at different energies due to their modified conjugated  $\pi$ -electron system [13], or from generated triplet states. For the latter, the dynamic range

is about three orders of magnitude slower than that of the investigated singlet exciton [14]. We also exclude effects by reabsorption as these are contradictory to the observed size-dependence of the PL intensity at 2.19 eV and as reabsorption should be strongly reduced at cryogenic temperatures by the smaller spectral overlap.

At first, the similar intensity enhancement with in-

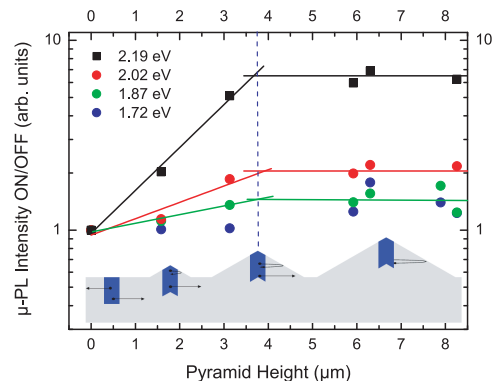


FIG. 2: Integrated PL intensity for various structure sizes normalized to that of the smooth rubrene surface. Pyramid heights above  $4 \mu\text{m}$  result in almost constant intensity ratios. This height coincides with the rubrene absorption length at 380 nm as illustrated by the shaded profiles in the sketch.

creasing structure size and the equidistant energy spacing suggest that the second set of peaks (2.02 eV, 1.87 eV, 1.72 eV) belongs to the same optical transition and its vibronic side-bands. The vibronic progression of the 2.02 eV peak (0-0 transition) indicates that the energy matches that of the rubrene C-C stretching mode of  $h\nu = 0.177 \text{ eV}$  [15]. In addition, the intensity decrease of the vibronic bands at lower energies agrees qualitatively with that expected from the Franck-Condon coefficients. However, to elucidate the strong enhancement of the total PL intensity from the microstructures, integrated over the entire energy range from 1.5 eV to 2.3 eV, a more sophisticated approach is needed to explain the underlying excitation processes. This again leads us to the assumption that the different emission bands may in fact not belong to the same vibronic structure but rather originate from two different excitonic species associated with the transitions at 2.19 eV and 2.02 eV. In particular, the 2.19 eV excitation is assigned to the formation of free excitons whereas the transition at 2.02 eV is associated to self-trapped excitons [14]. This idea is supported by luminescence studies on rubrene crystals and molecules in polymeric matrices, that show an intensity shift towards the 2.02 eV emission with increasing pressure [15]. Since the detection area corresponds to the PL excitation diameter of  $1 \mu\text{m}$ , we are primarily sensitive to excitons created and remaining within this area. *Vice versa*, excitons diffusing out of the focus will generally not con-

tribute to the measured peak intensities as only the parallel light coming from the focus of the infinity-corrected objective is sent back to the detectors. Using this constraint we are able to propose a possible scenario to rationalize the observed intensity enhancement under confined geometry as well as the resulting temperature dependence. If the exciton lifetime exceeds a certain value and, as a result, a certain diffusion length, the generated exciton can diffuse out of the focus in the case of the free rubrene surface and will therefore be undetectable. As, at 4 K, the decay time of the free exciton is on the order of about 4 ns (see Fig. 3) this would require an exciton diffusion constant of at least  $0.2 \text{ cm}^2/\text{s}$  assuming an isotropic 2D diffusion within the focal plane. A comparison with temperature dependent diffusion constants of  $10 \text{ cm}^2/\text{s}$ , reported e.g. for anthracene single crystals at 4 K [8], indicates a reasonable agreement keeping in mind that we deduced a lower limit for this value. In contrast, for the confined pyramidal structures one might expect a shifting of the HOMO and LUMO positions towards higher energies at the terminating facet planes due to the lower polarization energy at these surfaces. This effect is a consequence of missing next neighbors and a reduced polarization energy compared to that of the bulk [16]. Similar to single charge carriers, excitons approaching the facet surface experience a repelling potential at the boundary that reflects them back into the volume [17]. On average, the number of free excitons in the detection focus on the pyramids increases compared to that of the smooth surface. The self-trapped excitons are expected to be localized by lattice relaxation occurring on much shorter time scales of  $10^{-12}$  to  $10^{-11}$  s so that almost all generated excitons remain in the detection volume [7]. To further understand the intensity increase of the free exciton transition with the spatial extent of the pyramids the absorption characteristics of the respective structures have to be considered, as sketched in Fig. 2. As the rubrene absorption length for the excitation at 380 nm amounts to  $4 \mu\text{m}$  we conclude that for shallow pyramids, a substantial fraction of excitons is created in the bulk underneath. Due to extended diffusion in the (ab)-plane these excitons are not subjected to the confinement imposed by the microstructures. With increasing height, however, the absorption and thereby the generation of free excitons in the confined structures is continuously enhanced. By this model, the saturation of the PL intensity at 2.19 eV for pyramids of at least similar height than the rubrene absorption length becomes clear. Important questions raised by the PL spectra are: how does the conversion of the excited free exciton into the self-trapped state at elevated temperatures occurs and what is the related energy barrier? This phenomenon, which has been described in detail for several polyaromatic crystalline materials including rubrene [14, 18, 19, 20] will also be considered here with a special focus on the impact of the confined surface geometry. In

search of an indicator for such an energy transfer reaction, we have analyzed the temperature dependent exciton decay times. The experimental decay times in Fig. 3

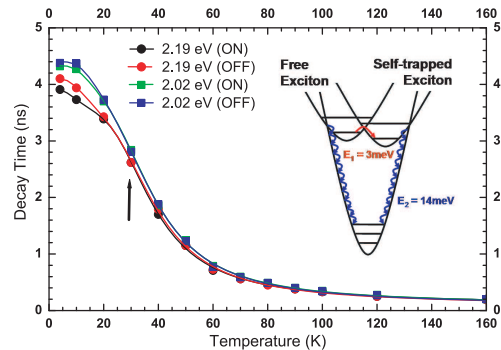


FIG. 3: Temperature dependent decay times for the 2.19 eV and the 2.02 eV emission (dots). As indicated by the arrow, above 30 K the decay times measured ON and OFF a microstructure coincide, whereas below 30 K a slight deviation occurs. The lines have been calculated according to Eq. (1).

show no significant differences between the two excitonic species at 2.19 eV and 2.02 eV down to 30 K for different topographic positions (ON/OFF). The similarity between the exciton dynamics measured on and off the microstructures can be explained by the strong exciton-phonon interaction, by which the free exciton gains sufficient energy to surmount the barrier to the self-trapped state. As further indicated by the identical decay times, rate-limited occupation is sustained in this temperature range [19]. Below 30 K, a divergence of about 500 ps between the decay times of the two excitonic states can be detected at an experimental error of 40 ps. To characterize the underlying microscopic processes, we have fitted the experimental data by a theoretical description including a radiative decay and two non-radiative decay channels, see e.g. [21]. This Boltzmann-type approach results in a temperature-dependent decay time

$$\tau(T) = \frac{1}{\gamma_r + \gamma_{nr1} \exp\left(-\frac{E_1}{k_B T}\right) + \gamma_{nr2} \exp\left(-\frac{E_2}{k_B T}\right)} \quad (1)$$

where  $\gamma_r$  is the inverse lifetime of the radiative transition and  $\gamma_{nr i}$  describes the rate of the non-radiative transition with activation energy  $E_i$ . The curves calculated accordingly (lines in Fig. 3) reproduce the experimental data satisfactorily, revealing activation energies for the non-radiative decay of  $E_1 \approx 3 \text{ meV}$  and  $E_2 \approx 14 \text{ meV}$ . Comparing the adjusted rates  $\gamma_r \approx 3 \cdot 10^8 \text{ s}^{-1}$ ,  $\gamma_{nr1} \approx 2 \cdot 10^8 \text{ s}^{-1}$  and  $\gamma_{nr2} \approx 10^{10} \text{ s}^{-1}$  directly indicates that channel 2 is the dominant (non-radiative) decay path. In this context, the high non-radiative decay rate  $\gamma_{nr2}$  describes the homogeneous quenching of all PL channels resulting in halving of  $\tau$  between 0 K and

30 K, whereas the low rate  $\gamma_{nr1}$  is only responsible for the deviation occurring in this temperature regime. As possible mechanisms related to the energies  $E_i$  we suggest an agreement of  $E_2$  with that of lowest-energy intermolecular optical phonon modes in such molecular solids. For instance, according to *ab-initio* density functional theory calculations on naphthalene this phonon branch occurs at energies between 10 and 20 meV [22]. Although no distinct microscopic processes could be attributed to the energy  $E_1$  yet, this value is in accordance with the barrier between free and self-trapped excitonic states reported for other perylene-derivatives, like PTCDA [21]. Finally, we have analyzed the temperature-dependent ratio between the intensities of the free and the self-trapped excitonic state as an additional measure for the relevant activation energy. Figure 4 shows the reciprocal temperature dependence of this ratio detected at ON and OFF positions. From the graph it is clear that for both positions the transition is thermally activated. The difference

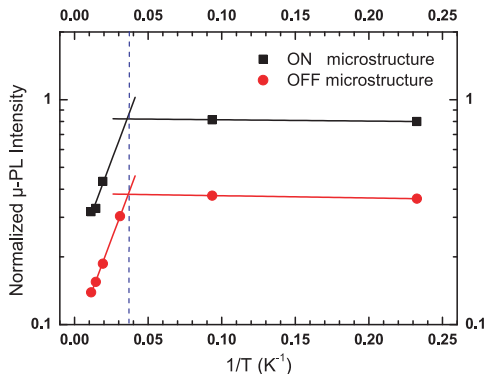


FIG. 4: Temperature depended intensity of the 2.19 eV emission normalized to the 2.02 eV emission including its vibronic replica. Below  $0.04 \text{ K}^{-1}$  the thermally activated transition yields an activation energy of 2 meV in accordance to  $E_1$ .

between the intensity ratios below 25 K (above  $0.04 \text{ K}^{-1}$ ) is again proposed to originate from the diffusion of free excitons out of the detection focus on the plane crystal surface compared to that under confined surface geometry. Above this temperature, both curves show a decrease in the area ratio. This is thought to evidence the efficient transfer of the free exciton into the self-trapped species. From the onset as well as from the linear slope we estimate an activation energy of 2 meV that is similar for the free surface and the confined geometry and confirms that estimated from the temperature dependent decay times. In conclusion, we have analyzed the optical properties of rubrene surface structures with confined geometries on the micrometer scale. The results were compared with the exciton generation and dynamics of the bare (001) crystal surface. We attribute the excitation to whether a free exciton or an exciton self-trapped by polarizing its

molecular environment is formed. Although both geometries show similar decay times and activation barriers, for the confined geometry the fraction of free excitons turned out to be strongly enhanced with respect to that of the plane rubrene surface. This effect is explained by the respective optical absorption profile of the pyramids by which we identified a minimum height of about  $4 \mu\text{m}$  to confine the generated excitons. We propose the reported self-organized surface structures to be suitable for application as high quality micro-resonators.

We acknowledge S. Hirschmann for assistance and the DFG for financial support (project FOR 730).

- 
- [1] A. S. Davydov, *Theory of Molecular Excitons* (Plenum Press, New York, 1971).
  - [2] D. S. Chemla and J. Zyss, *Nonlinear Optical Properties of Organic Molecules and Crystals. Vol. 1* (Academic Press, Inc., New York, 1987).
  - [3] D. Faltermeier, B. Gompf, M. Dressel, A. K. Tripathi, and J. Pflaum, *Phys. Rev. B* **74**, 125416 (2006).
  - [4] I. G. Hill, A. Kahn, Z. G. Soos, and R. A. Pascal, *Chem. Phys. Lett.* **327**, 181 (2000).
  - [5] P. Peumans, A. Yakimov, and S. R. Forrest, *J. Appl. Phys.* **93**, 3693 (2003).
  - [6] A. Matsui and H. Nishimura, *J. Phys. Soc. Jpn.* **49**, 657 (1980).
  - [7] E. A. Silinsh and V. Capek, *Organic Molecular Crystals. Interaction, Localization and Transport Phenomena* (American Institute of Physics Press, New York, 1994).
  - [8] T. S. Rose, R. Righini, and M. D. Fayer, *Chem. Phys. Lett.* **106**, 13 (1984).
  - [9] V. M. Kenkre and D. Schmid, *Phys. Rev. B* **31**, 2430 (1985).
  - [10] H. Kasai, H. Kamatani, S. Okada, H. Oikawa, H. Matsuda, and H. Nakanishi, *Jpn. J. Appl. Phys.* **35**, L221 (1996).
  - [11] D. Käfer and G. Witte, *Phys. Chem. Chem. Phys.* **7**, 2850 (2005).
  - [12] M. Kytka, A. Gerlach, F. Schreiber, and J. Kovac, *Appl. Phys. Lett.* **90**, 131911 (2007).
  - [13] O. Mitrofanov, D. V. Lang, C. Kloc, J. M. Wikberg, T. Siegrist, W. Y. So, M. A. Sergent, and A. P. Ramirez, *Phys. Rev. Lett.* **97**, 166601 (2006).
  - [14] H. Najafov, I. Biaggio, V. Podzorov, M. F. Calhoun, and M. E. Gershenson, *Phys. Rev. Lett.* **96**, 056604 (2006).
  - [15] T. T. Nakashima and H. W. Offen, *J. Chem. Phys.* **48**, 4817 (1968).
  - [16] W. R. Salaneck, *Phys. Rev. Lett.* **40**, 60 (1978).
  - [17] R. Merrifield, *J. Chem. Phys.* **28**, 647 (1958).
  - [18] R. Horiguchi, N. Iwasaki, and Y. Maruyama, *J. Phys. Chem.* **91**, 5135 (1987).
  - [19] H. Nishimura, T. Yamaoka, K. Mizuno, M. Iemura, and A. Matsui, *J. Phys. Soc. Jpn.* **53**, 3999 (1984).
  - [20] R. Scholz, A. Y. Kobitski, D. R. T. Zahn, and M. Schreiber, *Phys. Rev. B* **72**, 245208 (2005).
  - [21] A. Y. Kobitski, R. Scholz, D. R. T. Zahn, and H. P. Wagner, *Phys. Rev. B* **68**, 155201 (2003).
  - [22] K. Hannewald and P. A. Bobbert, *Appl. Phys. Lett.* **85**, 1535 (2004).